Probing Planckian physics: resonant production of particles during inflation and features in the primordial power spectrum

Daniel J. H. Chung[*]

Randall Physics Laboratory, University of Michigan, Ann Arbor, Michigan 48109-1120

Edward W. Kolb[†]

*NASA/Fermilab Astrophysics Center, Fermi National Accelerator Laboratory, Batavia, Illinois 60510-0500,
and Department of Astronomy and Astrophysics, Enrico Fermi Institute,
The University of Chicago, Chicago, Illinois 60637-1433*

Antonio Riotto[‡]

Theory Division, CERN, CH-1211 Geneva 23, Switzerland

Igor I. Tkachev[§]

*Theory Division, CERN, CH-1211 Geneva 23, Switzerland, and
Institute for Nuclear Research, Russian Academy of Sciences, Moscow 117312, Russia*

(September 1999)

The phenomenon of resonant production of particles *after* inflation has received much attention in the past few years. In a new application of resonant production of particles, we consider the effect of a resonance *during* inflation. We show that if the inflaton is coupled to a massive particle, resonant production of the particle during inflation modifies the evolution of the inflaton, and may leave an imprint in the form of sharp features in the primordial power spectrum. Precision measurements of microwave background anisotropies and large-scale structure surveys could be sensitive to the features, and probe the spectrum of particles as massive as the Planck scale.

I. INTRODUCTION AND MOTIVATION

Analysis of the statistics of temperature fluctuations of the cosmic background radiation (CBR) and the distribution of galaxies and galaxy clusters in large-scale structure (LSS) surveys yield the presently observed power spectrum of scalar density perturbations. The power spectrum is a most useful and fundamental tool for understanding the origin and development of the large-scale structure of the universe.

It is likely that the observed power spectrum had a primordial origin, resulting from events that occurred in the early universe. The primordial power spectrum is not directly observable since it is adulterated by a variety of cosmological and astrophysical processes associated with the transition from a radiation-dominated to a matter-dominated universe, with the decoupling of matter and radiation, with the free streaming of dark matter, and so on. Nevertheless, present observations of the power spectrum allow us to infer the form of the primordial power spectrum.

To a first approximation, present observations of the power spectrum are consistent with it having originated from a primordial power spectrum that is featureless, i.e., a primordial spectrum of the form k^n where k is the wavenumber and n is the spectral index. However, there are hints of features in the power spectrum from analysis of the Automatic Plate Measurement (APM) survey [1], from apparent regularity in the redshift distribution of galaxies seen in deep pencil-beam surveys [2], cluster redshift surveys [3], and galaxy surveys [4,5].

There are (at least) three possible responses to these "hints." The first response is that the apparent features are an artifact of small data sets or data sets with systematic errors, and the effects will eventually disappear with better or more complete observations. Another possibility is that the features are real, and they reflect the shape of the

---

[*]Electronic mail: djchung@umich.edu

[†]Electronic mail: rocky@rigoletto.fnal.gov

[‡]Electronic mail: riotto@nxth04.cern.ch

[§]Electronic mail: Igor.Tkachev@cern.ch

primordial power spectrum. A third response is that the primordial power spectrum is smooth, but astrophysical processing of the primordial power spectrum produces the features.

A well known example of the last phenomenon is the "Zel'dovich peaks" in the angular power spectrum of CBR temperature fluctuations. The peaks are not believed to reflect features in the primordial power spectrum, but presumably result from astrophysical processing, in this case, acoustic oscillations of the baryon–photon fluid. However, the features in the matter power spectrum around $100h^{-1}$ Mpc are not well fit by acoustic oscillations [6].

The leading theory for the origin of the primordial power spectrum is quantum fluctuations during inflation. Simple models of inflation produce a featureless, nearly exact power-law spectrum of primordial perturbations. Of course, an important qualifier in the previous sentence is "simple." A variety of inflation models that produce features in the primordial spectrum have been studied. These include variants of extended inflation [7] that produce rare large voids [8], models with multiple episodes of inflation [9], and phase transitions during the inflationary phase [10].

In this paper we propose a mechanism to produce features in the primordial power spectrum by a very simple variant of the simplest inflation model. Our basic idea is to couple the inflaton to a massive particle, with resonant production of the particle during inflation. Resonant extraction of even a small fraction of the energy of the inflaton field during inflation can alter the classical motion of the inflaton and produce features in the primordial power spectrum.

The primordial power spectrum is most conveniently expressed in terms of the amplitude of the density perturbation when it crosses the Hubble radius after inflation, $\delta_H(k)$. For reference, the Harrison–Zel'dovich spectrum has $\delta_H(k)$ independent of k. A qualitative feel for our mechanism can be obtained by recalling the simple approximation for the density perturbations produced during inflation [11],

$$\delta_H(k) \sim \frac{H^2}{5\pi\dot{\phi}} \ . \tag{1}$$

Here, H is the expansion rate of the universe and $\dot{\phi}$ is the velocity of the inflaton field when the comoving wavenumber k crossed the Hubble radius during inflation. We find that resonant extraction of inflaton field energy decreases $\dot{\phi}$, leading to an increase in $\delta_H(k)$. Because of the resonant nature of the process, the produced feature is rather sharp, extending less than a decade in wavenumber.

There are two reasons why our study may be important. The first reason is that features in the observed power spectrum have important astrophysical implications. Fitting the CBR Zel'dovich peaks is an important part of cosmological parameter estimation [12]. Spurious peaks in the spectrum arising from resonant particle production will complicate the extraction of parameters (although joint parameter estimation from CBR and LSS [13] may help alleviate the problem).

If baryons are a relatively large fraction of the matter density, the effect of acoustic oscillations on the matter power spectrum [13,14] may be seen in accurate determinations of the power spectrum in the next generation of large-scale structure surveys such as the 2-degree Field project [15] and the Sloan Digital Sky Survey (SDSS) [16], and may be part of the parameter estimation program [17]. Again, this program is complicated if the primordial perturbation spectrum does not have a smooth power law form [18]. Finally, the program of reconstruction of the inflaton potential from CBR and large-scale structure determinations of the power spectrum [19–21] may be compromised if there are sharp features.

The second reason we believe our study is relevant is that peaks in the primordial power spectrum may serve as a probe of energy scales as large as the Planck scale. We will discuss the particle physics motivation for the coupling and masses of the particles in a later section. But to see the possibility of probing Planck-scale physics, simply assume a chaotic inflation model with a quadratic potential. The inflaton mass in this model is around 10^{13} GeV, which is also approximately the expansion rate of the universe during inflation. During inflation the value of the inflaton field is a few times the Planck mass, m_{Pl}. Since the energy density during the inflationary stage is of the order of $m_\phi^2 m_{Pl}^2 \ll m_{Pl}^4$, in the spirit of effective field theories we may regard the inflaton potential as the low-energy limit of some fundamental Planck-scale theory. Furthermore, values of the the inflaton field $\phi \sim m_{Pl}$ do not necessarily lead to a breakdown of the field theory expansion; for example, moduli fields in superstring theories whose vacuum expectation values parameterize different string vacua usually have field values of the order of the Planck scale.

The inflaton may be coupled to other degrees of freedom with mass a few times the Planck mass, but these degrees of freedom are usually integrated out and do not appear in the low-energy action. Of relevance for our considerations is the possibility that the inflaton field couples to a particle of mass a few times the Planck mass. Normally, the massive particle would be integrated out and not affect the low-energy theory. In the inflaton models we study, observable length scales exit the Hubble radius during inflation when the value of the inflaton field is a few times the Planck mass. If the inflaton couples to a fermion of mass m (assumed to be of order of m_{Pl}) with Yukawa coupling

λ, then the ϕ-dependent mass of the fermion is $M(\phi) = m - \lambda\phi$.[1] The ϕ ground state is $\phi = 0$, and in the ground state the fermion is supermassive and not part of the effective low-energy theory. But when $\phi \simeq m/\lambda$, the effective mass of the fermion vanishes, and it cannot be integrated out. When $\phi \simeq \phi_* = m/\lambda$ and the fermions are light, and they can be efficiently produced [22]. Since $\phi \gtrsim m_{Pl}$ during inflation, it can act as a probe of Planckian physics.

Ours is not the first study of parametric creation of fermions. Pure gravitational creation was considered in Refs. [23,24]. Creation by an oscillating background field in Minkowski space was considered in Refs. [25,26]. Resonant production of *massless* fermions *after* inflation (i.e., during preheating) in a $\lambda\phi^4$ inflation model was studied by Greene and Kofman [28]. Non-thermal productions of gravitinos have been considered in Ref. [27]. Finally, resonant production of *massive* fermions during preheating *after* inflation in an $m_\phi^2\phi^2$ inflation model was considered by Giudice, Peloso, Riotto, and Tkachev [22]. We draw heavily from the results in these important papers. The new twist we present is a change in the venue for particle production: we assume the resonance occurs *during* inflation. We believe this may be the most easily tested possibility because it leads to directly observable effects in the power spectrum.

In the next section we will provide more details about the couplings in the model we study and discuss the basics of resonant particle creation during inflation. In Sec. III we consider resonant production where back reactions are not important. We make some analytic approximations leading to an estimate of the effect on the density perturbation spectrum. In Sec. IV we present the results of a numerical calculation of the perturbation spectrum including the effect of resonant particle creation in the regime where back reactions are important. In Sec. V we discuss the prospect of detection of the type of features we produce. Finally we present a brief summary in the concluding section.

II. HEAVY PARTICLE PRODUCTION DURING INFLATION

Resonant particle production can occur for a range of choices of inflation models as well as different heavy particle masses and couplings of the massive state to the inflaton. We will develop analytic techniques and present numerical results for one model, and mention the generalization of our results where appropriate.

We will assume that the inflaton potential during inflation is given by a simple quadratic potential of the form

$$V(\phi) = \frac{1}{2}m_\phi^2\phi^2 \ . \tag{2}$$

The value of the inflaton mass can be fixed by normalization of the perturbation spectrum, with result $m_\phi = 10^{13}$ GeV. Inflation occurs for Planckian values of the inflaton field, $\phi \gtrsim m_{Pl}$, where m_{Pl} is the Planck mass. Inflation ends when $\phi \sim 0.2 m_{PL}$, and scales relevant for CBR fluctuations and large-scale structure studies cross the Hubble radius during inflation when ϕ is in the range of approximately $2m_{Pl}$ to $3m_{Pl}$.

Now we will couple a fermion ψ of mass M to the inflaton by a Yukawa term of the form[2]

$$\mathcal{L}_Y = -\lambda\phi\bar{\psi}\psi \ . \tag{3}$$

If ϕ is nonzero, then the effective mass of the fermion is[3]

$$M(\phi) = m - \lambda\phi \ . \tag{4}$$

These choices lead to a critical value of the inflaton field, which we will denote as ϕ_*, where the effective mass of the fermion vanishes:

$$\phi_* = m/\lambda \ . \tag{5}$$

Resonant fermion production will occur in a narrow interval around $\phi = \phi_*$ [22].

---

[1]The important feature here is that the ϕ-dependent mass vanish during inflation. This can be accomplished by choosing a negative sign for the Yukawa term, or by taking ϕ to be negative. In this paper we will choose positive value of ϕ and a negative Yukawa term. An important notational convention is the distinction between m and $M(\phi) = m - \lambda\phi$.

[2]Here we treat a Dirac fermion, but there is no qualitative difference if one chooses Majorana fermions.

[3]Notice that radiative corrections from the heavy fermion may spoil the flatness of the inflaton potential. As usual, one can invoke supersymmetry to preserve the flatness. If this is the case and the starting superpotential is $2W = m_\phi\phi^2 + (m - \lambda\phi)\psi^2$, it is easy to show that radiative corrections are negligible, with the one-loop effective potential $32\pi^2 V_1 \simeq \lambda^2 m_\phi^2\phi^2 \log(\lambda^2\phi^2/\Lambda^2)$, where Λ is the renormalization scale.

3

Although we chose a fermion for the massive state, one might imagine that the massive state is a boson. Recall that the requirement for particle production is that the effective mass term goes through zero at ϕ_*. If the effective mass term goes through zero, then one might expect that it is negative either above or below ϕ_*. Since the sign of a fermion mass term is irrelevant, a negative mass term is not a problem. If the massive state is a boson, then the quadratic nature of the mass term implies one has to worry about tachyonic modes. So if the massive state is a boson, then the effective mass term should remain positive both above and below ϕ_*. This can be done, for instance, by taking a boson σ with potential $V(\sigma) = \sigma^2 (m_\sigma - g\phi)^2 + \lambda_\sigma \sigma^4$, where $m_\sigma > 0$. The vacuum expectation value of the field σ vanishes. The effective mass term of the boson, $M_\sigma^2 = 2 (m_\sigma - g\phi)^2$, remains positive definite and vanishes at $\phi_* = m_\sigma/g$.

Now consider fermion production. In an expanding universe, the fermion field ψ satisfies the Dirac equation in conformal time η $(ad\eta = dt)$,

$$\left(\frac{i}{a}\slashed{\partial} + i\frac{3}{2}H\gamma^0 - M \right) \psi = 0 \ , \tag{6}$$

where a is the scale factor, γ^μ are the flat-space gamma matrices, the spatial derivatives are with regard to comoving coordinates, and the Hubble expansion rate is $H = \dot{a}/a = a'/a^2$ (here and throughout the paper a prime superscript implies $d/d\eta$). This equation can be reduced to a more familiar form of the Dirac equation by defining a new field $\chi = a^{-3/2}\psi$. In terms of the new field χ, the Dirac equation in an expanding universe becomes

$$[i\slashed{\partial} - a(\eta)M(\eta)]\chi = 0 \ . \tag{7}$$

Of course M depends on η through the dependence of ϕ on η.

The field χ can be expanded in terms of Fourier modes of the form

$$\chi(x) = \int \frac{d^3k}{(2\pi)^{3/2}} \ e^{-i\vec{k}\cdot\vec{x}} \sum_{r=\pm 1} \left[u_r(k,\eta)a_r(k) + v_r(k,\eta)b_r^\dagger(-k) \right] \ , \tag{8}$$

where the summation is over spin and $v_r(k) \equiv C\bar{u}_r^T(-k)$. The canonical anticommutation relations imposed upon the creation and annihilation operators may be used to normalize the spinors u and v.

Defining $u_r \equiv [u_+(\eta)\psi_r(k), ru_-(\eta)\psi_r(k)]^T$ and $v_r \equiv [rv_+(\eta)\psi_r(k), v_-(\eta)\psi_r(k)]^T$, where $\psi_r(k)$ are the two-component eigenvectors of the helicity operators, and using a representation where $\gamma^0 = \text{diag}(\mathbb{1}, -\mathbb{1})$, Eq. (8) can be written as two uncoupled second-order differential equations for u_+ and u_-:

$$u_\pm'' + \left[\omega_k^2 \pm i(aM)'\right] u_\pm = 0 \ , \tag{9}$$

where, $\omega_k^2(\eta) = k^2 + M^2(\eta)a^2(\eta)$ and $M(\eta) = m - \lambda\phi(\eta)$. Notice that the normalization conditions $u_r^\dagger u_s = v_r^\dagger v_s = 2\delta_{rs}$ and $u_r^\dagger v_s = 0$ are preserved during the evolution. Furthermore, sometimes it is useful to remember that v_+ has the same evolution as $-u_-^*$ and v_- has the same evolution as u_+^*.

In order to calculate the number density, we must first diagonalize the Hamiltonian. In the basis of Eq. (8) the Hamiltonian is

$$H(\eta) = \int d^3k \sum_r \left\{ E_k(\eta) \left[a_r^\dagger(k)a_r(k) - b_r(k)b_r^\dagger(k) \right] + F_k(\eta)b_r(-k)a_r(k) + F_k^*(\eta)a_r^\dagger(k)b_r^\dagger(-k) \right\} \ , \tag{10}$$

where the equations of motion can be used to express E_k and F_k in terms of u_+ and u_-:[4]

$$E_k = k\text{Re}(u_+^* u_-) + aM \left(1 - |u_+|^2 \right) \ ,$$
$$F_k = \frac{k}{2}(u_+^2 - u_-^2) + aMu_+u_- \ . \tag{11}$$

In order to calculate particle production one wants to write the Hamiltonian in terms of creation and annihilation operators that are diagonal. To do this one defines a new set of creation and annihilation operators, $\hat{a}$ and $\hat{b}^\dagger$, related

---

[4]Here we choose the momentum k along the third axis and use the representation in which $\gamma^3 = \begin{pmatrix} 0 & \mathbb{1} \\ -\mathbb{1} & 0 \end{pmatrix}$.

to the original creation and annihilation operators a and $b^\dagger$ through the (time-dependent) Bogolyubov coefficients α_k and β_k,

$$\hat{a}(k) = \alpha_k(\eta)a(k) + \beta_k(\eta)b^\dagger(-k) \,,$$
$$\hat{b}^\dagger(k) = -\beta_k^*(\eta)a(k) + \alpha_k^*(\eta)b^\dagger(-k) \,. \tag{12}$$

The Bogolyubov coefficients will be chosen to diagonalize the Hamiltonian. Using the fact that the canonical commutation relations imply $|\alpha_k|^2 + |\beta_k|^2 = 1$, the choice

$$\frac{\alpha_k}{\beta_k} = \frac{E_k + \omega_k}{F_k^*} \,, \quad |\beta_k|^2 = \frac{|F_k|^2}{2\omega_k(\omega_k + E_k)} \,, \tag{13}$$

results in a diagonal Hamiltonian,

$$H(\eta) = \int d^3k \sum_r \omega_k(\eta) \left[\hat{a}_r^\dagger(k)\hat{a}_r(k) + \hat{b}_r^\dagger(k)\hat{b}_r(k) \right] \,. \tag{14}$$

We define the initial vacuum state $|0\rangle$ such that $a|0\rangle = b|0\rangle = 0$. The initial conditions corresponding to the no-particle state are

$$u_\pm(0) = \sqrt{\frac{\omega_k \mp Ma}{\omega_k}} \,; \qquad u'_\pm(0) = iku_\mp(0) \mp iaMu_\pm(0) \,. \tag{15}$$

The (quasi) particle number operator can be defined as $\mathcal{N} = \hat{a}_r^\dagger(k)\hat{a}_r(k)$, and the particle number density n is (including the two degrees of freedom from the spin)

$$n(\eta) = \langle 0 | \mathcal{N}/V | 0 \rangle = \frac{1}{\pi^2 a^3(\eta)} \int_0^\infty dk \, k^2 \, |\beta_k|^2 \,. \tag{16}$$

An equal amount of antiparticles is produced.

Including the coupling of the fermion to the inflaton, the inflaton equation of motion in the Hartree approximation is

$$\ddot{\phi} + 3H\dot{\phi} + \frac{dV}{d\phi} - N\lambda\langle\bar{\psi}\psi\rangle = 0 \,, \tag{17}$$

where we have generalized to the case of N fermions of bare mass m coupled to the inflaton.

The product $\langle\bar{\psi}\psi\rangle$ can be expressed as momentum integration of the mode functions using the field decomposition, Eq. (8). A straightforward averaging leads to ultraviolet divergences, therefore, the quantity $\langle\bar{\psi}\psi\rangle$ must be regularized. As in the case of Minkowski spacetime, the regularization amounts to normal ordering or, equivalently, to the subtraction of zero-point vacuum fluctuations. To obtain a finite result, it is necessary to express the operator $\bar{\psi}\psi$ in normal-ordered form and subtract the part due to vacuum fluctuations. The normal-ordered $\bar{\psi}\psi$ operator has the form

$$N_\eta\left(\bar{\psi}\psi\right) \equiv \bar{\psi}\psi - \langle 0_\eta|\bar{\psi}\psi|0_\eta\rangle \,, \tag{18}$$

where the vacuum $|0_\eta\rangle$ is defined by

$$\hat{a}|0_\eta\rangle = \hat{b}|0_\eta\rangle = 0 \,. \tag{19}$$

The vacuum averaging in Eq. (17) is defined as averaging with respect to the original vacuum state (we remind the reader that we are working in the Heisenberg representation)

$$\langle\bar{\psi}\psi\rangle \equiv \langle 0|N_\eta\left(\bar{\psi}\psi\right)|0\rangle \,. \tag{20}$$

Using the operator redefinitions given in Eq. (12), it is straightforward to show that

$$\langle\bar{\psi}\psi\rangle = \frac{4}{(2\pi a)^3} \int d^3k \left[\left(|u_+|^2 - 1\right)|\beta_k|^2 + \mathrm{Re}\left(\alpha_k\beta_k^* u_+^* u_-^*\right) \right] \,. \tag{21}$$

Making use of the formulae in Eq. (13), we arrive at the following expression for the regularized average of $\bar{\psi}\psi$:

5

$$\langle \bar{\psi}\psi \rangle = \frac{2}{(2\pi a)^3} \int d^3k \left(|u_+|^2 + \frac{Ma}{\omega_k} - 1 \right) . \tag{22}$$

In the case of Majorana spinors the numerical factor is half that of Eq. (22).

We will use Eq. (22) when integrating the equation of motion [given in Eq. (17)] for the inflaton field. We have also consistently included the contribution from $\langle \bar{\psi}\psi \rangle$ in the equation of state when integrating Einstein's equations for the scale factor. We integrated the system of all equations in the conformal frame with Eq. (9) the equation of motion for the mode functions. For the case of an inflaton potential given by Eq. (2), Eq. (17) takes the form

$$\varphi'' + \left(m_\phi^2 a^2 - \frac{a''}{a} \right) \varphi - a^3 N \lambda \langle \bar{\psi}\psi \rangle = 0 , \tag{23}$$

where $\varphi \equiv a\phi$.

At this point it is useful to discuss the unknown parameters of the calculation. First, we do not know the inflaton potential (V). We simply assume it is a quadratic large-field model for the purposes of detailed calculations and return to this issue in a later section. We do not know the mass of the fermion (m) and the Yukawa coupling of the fermion to the inflaton (λ). We will assume that m and λ are such that ϕ_*, defined in Eq. (5), falls in the range of ϕ that corresponds to the epoch of inflation when astrophysically accessible scales are crossing the Hubble radius. In the large-field inflation model we study, this corresponds to m/λ a few times the Planck mass. Particle production is most efficient when λ is large, so m also must be large to have ϕ_* in the relevant region. Finally, we do not know the number of fermion fields that couple to the inflaton (N). This number is potentially very large because there are often fermion representations of large dimension in superunified theories. So with the assumption of the large-field quadratic inflation model, the parameter space is spanned by $\{m, \lambda, N\}$, with the ratio m/λ reasonably well constrained.

III. ANALYTIC APPROXIMATIONS AND NUMERICAL RESULTS WHEN BACK REACTIONS ARE UNIMPORTANT

If only a small fraction of inflaton energy is extracted in resonant production of particles, then it is possible to find reasonably accurate analytic approximations for the features produced in the primordial perturbation spectrum.

There are three steps in obtaining analytic approximations for the modification to the perturbation spectrum due to resonant particle production during inflation. The first step is to determine the efficiency of resonant fermion production. The next step is to estimate the effect of fermion production on $\dot{\phi}$. Finally, it is necessary to convert a change in $\dot{\phi}$ to the modification of the perturbation spectrum.

A. Fermion Production

First consider the question of particle production. Start with the wave equation, Eq. (9):

$$u_\pm'' + (k^2 + M^2 a^2)u_\pm \pm i(aM)' u_\pm = 0. \tag{24}$$

Now define the (conformal) time η_* to be the time when $M(\eta_*) = 0$. Recalling that $M = m - \lambda\phi$, in the vicinity of $\eta = \eta_*$ we may expand $M(\eta)$ as

$$M(\eta) = \lambda\phi_*'(\eta - \eta_*) + \cdots , \tag{25}$$

where $\phi_*' \equiv \phi'(\eta_*)$. Now let's assume that resonant production happens in a very narrow region of conformal time and the scale factor does not change much during particle production (i.e., $a' = 0$). Choosing $a_* \equiv a(\eta_*) = 1$, then around η_* the wave equation is

$$u_\pm'' + \left[k^2 + \lambda^2 \phi_*'^2 (\eta - \eta_*)^2 \right] u_\pm \mp i\lambda\phi_*' u_\pm = 0 . \tag{26}$$

Now defining new variables $p = k/\sqrt{\lambda\phi_*'}$, $\tau = \sqrt{\lambda\phi_*'}(\eta - \eta_*)$, and denoting $d/d\tau$ by a dot, the wave equation becomes

$$\ddot{u}_\pm + \left(p^2 \mp i + \tau^2 \right) u_\pm = 0 . \tag{27}$$

The solutions to this equation are the parabolic cylinder functions. Choosing the boundary conditions associated with the no-particle initial state, one can estimate the phase-space density of the created particles to be (cf. the Bosonic case discussed in Refs. [29–31])

$$|\beta_k|^2 \simeq \exp\left(-\frac{\pi k^2}{\lambda|\phi'_*|}\right) \ . \tag{28}$$

The argument of the exponential appearing in Eq. (28) can be expressed in terms of a physical momentum, k_p, the time derivative of the inflaton field, and the expansion rate at resonance, as

$$\frac{\pi k^2}{\lambda \phi'_*} = \frac{\pi}{\lambda} \frac{H_*^2}{|\dot\phi_*|} \left(\frac{k_p}{H_*}\right)^2 \ . \tag{29}$$

Here H_* is the Hubble expansion rate and $\dot\phi_*$ is the unperturbed velocity of the inflaton field at $\eta = \eta_*$.
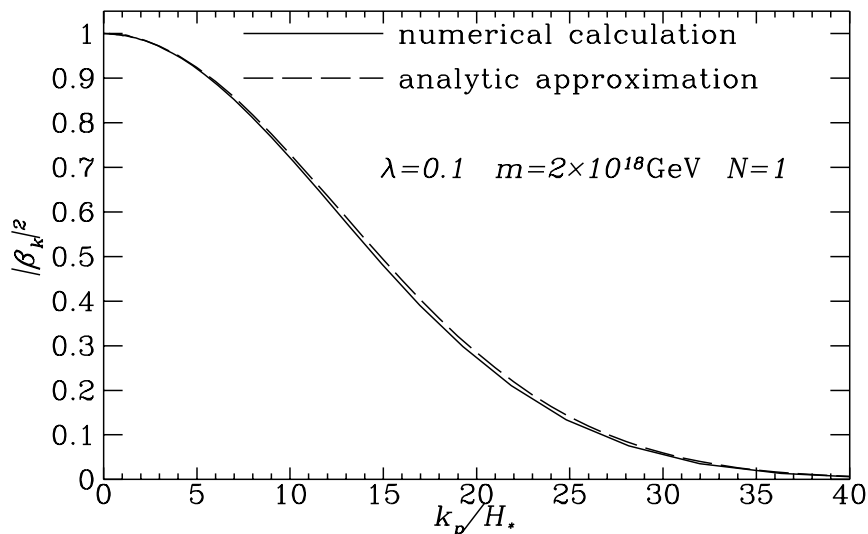
FIG. 1. The spectrum of produced fermions around $\eta = \eta_*$ as a function of physical momentum k_p. Also shown is the analytic approximation.

If the resonance occurs at $\phi_* \simeq 2m_{Pl}$, then $H_* \simeq 4m_\phi$ and $|\dot\phi| \simeq 0.16m_{Pl}m_\phi$. The crucial fact is that in this model the ratio $H_*^2/|\dot\phi_*|$ is very small, about 10^{-4}. This allows the phase-space density to be large in regions where the physical momentum is larger than the inverse of the Hubble radius. The smallness of this ratio should obtain in all slow-roll inflation models.

Fig. 1 shows an example of the comparison between the analytic formula of Eq. (28) and a numerical solution of the equations. The momentum is in units of k_p/H_*, where k_p is the physical momentum at the time η_*.

There are two important results one may learn from Fig. 1. The first is that the analytic approximation is quite accurate. The second important fact is that, as expected from the discussion above, the phase-space density is large for k greater than H_*.[5] This means that the effect is dominated by sub-Hubble-radius wavelength modes.

The physical number density of each Dirac fermion species (particles plus antiparticles for a total of four degrees of freedom) produced at η_* is given by

$$n(\eta_*) = \frac{2}{\pi^2} \int_0^\infty dk_p \, k_p^2 \, |\beta_k|^2 = \frac{\lambda^{3/2}}{2\pi^3} \left(\frac{|\dot\phi_*|}{H_*^2}\right)^{3/2} H_*^3 \ . \tag{30}$$

For $\eta \geq \eta_*$, the number density of fermions simply decreases as a^{-3}. For $\eta > \eta_*$ the fermion mass is approximately m, so knowing the number density at $\eta = \eta_*$ allows us to estimate the contribution of the produced fermions for $\eta > \eta_*$.

---

[5]The contribution per logarithmic interval in k is proportional to $k^3|\beta_k|^2$, so the peak contribution to the number density of created particles occurs for $k_p \gg H_*$.

B. Inflaton Velocity

Now we turn to the issue of how resonant production of the fermions modifies $\dot{\phi}$. Let's start with the equation of motion for the inflaton field, Eq. (17). Here we are interested in change in the velocity of the inflaton field caused by particle creation. Consider a small region around the time of particle creation, $t = t_*$. In this small region $H = H_*$ and $dV/d\phi = (dV/d\phi)_*$ are approximately constant.

We may also approximate $\langle \bar{\psi}\psi \rangle$ by assuming the number density of fermions is zero before t_*, equal to $n_* \equiv n(\eta_*)$ [given by Eq. (30)] at $t = t_*$, and decreases as a^{-3} thereafter:

$$\langle \bar{\psi}\psi \rangle = n_* \, \theta(t - t_*) \left(\frac{a_*}{a} \right)^3 \simeq n_* \, \theta(t - t_*) \, \exp[-3H_*(t - t_*)] \ . \tag{31}$$

Here for simplicity we assume an exponential growth of the scale factor during inflation.

The fact that $\langle \bar{\psi}\psi \rangle$ can be approximated by n_* may be understood as follows. The mode functions have an adiabatic evolution before and after the time η_* when $M(\eta_*) = 0$. The nonadiabatic changes of the mode functions occur only in the vicinity of η_*. Therefore we expect the mode function

$$u_+(\eta < \eta_*, k) = \sqrt{1 - \frac{Ma}{\omega_k}} \, \exp\left(-i \int^\eta \omega_k \, d\eta \right) \tag{32}$$

to be the adiabatic solution of Eq. (9) before the particle production at time η_*. After the production time, the mode function u_+ is again an adiabatic solution, with the difference that it picks up a negative frequency. It may be expressed in the form

$$u_+(\eta > \eta_*, k) = \alpha_k \sqrt{1 - \frac{Ma}{\omega_k}} \, \exp\left(-i \int^\eta \omega_k \, d\eta \right) - \beta_k \sqrt{1 + \frac{Ma}{\omega_k}} \, \exp\left(+i \int^\eta \omega_k \, d\eta \right) \ . \tag{33}$$

Inserting this expression into Eq. (22) and making use of the property $|\alpha_k|^2 + |\beta_k|^2 = 1$, we obtain

$$\langle \bar{\psi}\psi \rangle = \frac{4}{(2\pi a)^3} \int d^3k \left\{ \frac{Ma}{\omega_k} |\beta_k|^2 - \frac{k}{\omega_k} \text{Re}\left[\alpha_k \beta_k^* \exp\left(-2i \int^\eta \omega_k \, d\eta \right) \right] \right\} \ . \tag{34}$$

The Bogolyubov coefficient $|\beta_k|^2$ may be well approximated by unity for $k \lesssim k_* = \sqrt{\lambda |\phi_*'|}$ and zero otherwise. Furthermore, at $\eta > \eta_*$ it is safe to neglect the inflaton field dependent part in the mass M of the fermion ψ and we have $M \simeq m \gg k_*$. Under these circumstances, Eq. (34) reduces to

$$\langle \bar{\psi}\psi \rangle = \frac{4}{(2\pi a)^3} \int d^3k \left(\frac{Ma}{\omega_k} |\beta_k|^2 \right) \simeq \frac{4}{(2\pi a)^3} \int d^3k \, |\beta_k|^2 \equiv n_* . \tag{35}$$

This proves that $\langle \bar{\psi}\psi \rangle$ can be approximated by n_*.

With this approximation for $\langle \bar{\psi}\psi \rangle$, the first-order differential equation for $\dot{\phi}$ [Eq. (17)] is

$$\frac{d\dot{\phi}}{dt} + 3H_* \dot{\phi} + (dV/d\phi)_* - N\lambda n_* \theta(t - t_*) \exp[-3H_*(t - t_*)] = 0 \ . \tag{36}$$

The solution of this equation for $t > t_*$ is

$$\dot{\phi}(t > t_*) = \dot{\phi}_* \exp[-3H_*(t - t_*)] - \frac{(dV/d\phi)_*}{3H_*} \{ 1 - \exp[-3H_*(t - t_*)] \} + N\lambda n_* (t - t_*) \exp[-3H_*(t - t_*)] \ . \tag{37}$$

We may easily calculate the change in $\dot{\phi}$ due to particle creation:

$$\Delta \dot{\phi}(t > t_*) = \dot{\phi}(t > t_*) - \left[\dot{\phi}(t > t_*) \right]_{\lambda=0} = N\lambda n_* (t - t_*) \exp[-3H_*(t - t_*)] \ . \tag{38}$$
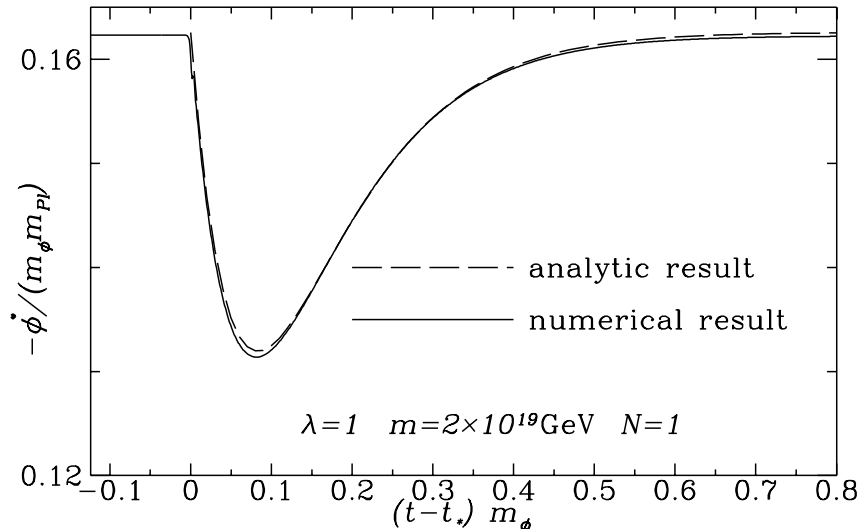
8

FIG. 2. The numerical result for the evolution of $\dot{\phi}$, including the effect of resonant particle production, is shown by the solid curve. Also shown by the dashed curve (nearly indistinguishable from the numerical result) is the analytic expression of Eq. (38).

The maximum size of the feature can also be estimated. Equation (38) has a maximum at $t = (3H_*)^{-1}$ of

$$\frac{\max[\Delta\dot{\phi}]}{m_{Pl}m_\phi} = \frac{\Delta\dot{\phi}(t=1/3H_*)}{m_{Pl}m_\phi} = \frac{N\lambda^{5/2}}{6e\pi^3}\frac{|\dot{\phi}_*|^{3/2}}{H_*m_{Pl}m_\phi} \ , \tag{39}$$

where we have used Eq. (30) for n_*.

In Fig. 2 we present the result of a numerical calculation. Note that $\max[\Delta\dot{\phi}]$ is about $0.03m_{Pl}m_\phi$. For the model of Fig. 2, $H_* \simeq 4m_\phi$ and $\dot{\phi}_* \simeq 0.16m_{Pl}m_\phi$, and from Eq. (39) we predict $\max[\Delta\dot{\phi}] \simeq 0.03m_{Pl}m_\phi$, in excellent agreement with the numerical results. Not just the depth of the feature, but the entire shape of the feature is well approximated by Eq. (38).

We have assumed that the fermion is stable, or at least has a lifetime long compared to the time it takes to form the feature, $t - t_* \simeq 0.2m_\phi^{-1}$. This is not unreasonable at all. Indeed, in spite of the fact that the bare mass of the fermion is much larger than the inflaton mass, the fermions are produced when they are massless. Suppose we parameterize the decay rate of the fermion field by $\Gamma = \alpha M$, where α is a perturbative constant smaller then unity. Using the expansion of Eq. (25) and imposing the condition $\Gamma \gtrsim H$, we estimate that the fermions decay at time t_D such that $t_D - t_* \simeq (\lambda\alpha\phi_*)^{-1}$. The fermionic decays take place after the formation of the features in the spectrum if $t_D - t_* \gtrsim 0.2m_\phi^{-1}$. This amounts to requiring $\alpha \lesssim (5/\lambda)(m_\phi/\phi_*)$, which is not very restrictive. Another option is that the perturbative decay rate Γ identically vanishes for kinematical reasons at the inflationary stage. This will happen if the particles coupled to the fermion ψ are heavier than the mass of the ψ during inflation.

In the opposite extreme, $\Gamma \ll H_*$, we may assume that the fermions decay very soon after they are produced. In this case, the factor of $\exp[-3H_*(t - t_*)]$ in Eq. (31) would be modified. Again using the fact that around the resonance $M \simeq \lambda\dot{\phi}_*(t - t_*)$, the factor becomes $\exp[-3H_*(t - t_*)]\exp[-\alpha\lambda\dot{\phi}_*(t - t_*)^2]$. One can follow through and derive a similar analytic approximation to $\Delta\dot{\phi}$ [cf. Eq. (38)],

$$\Delta\dot{\phi} = N\lambda n_* \exp[-3H_*(t - t_*)]\frac{1}{\sqrt{\alpha\lambda\dot{\phi}_*}}\frac{\sqrt{\pi}}{2}\,\text{erf}\left[\sqrt{\alpha\lambda\dot{\phi}_*}(t - t_*)\right] \ . \tag{40}$$

Of course in the limit that the particle is stable, $\alpha \to 0$, the error function may be expanded to recover Eq. (38). The decay of the massive state results in a feature that is narrower and less pronounced than if the massive particle energy density decreases simply as matter (see Fig. 3). The feature in $\dot{\phi}$ will map onto the feature in δ_H as discussed in the next section.

We do not know the relevant value of α, but if we choose a random value, say $\alpha = (137)^{-1}$, then $\sqrt{\alpha\lambda\dot{\phi}_*} = 34$ for $\lambda = 1$. This would make a few percent change in the amplitude of the feature and make it a bit narrower (see Fig. 3).
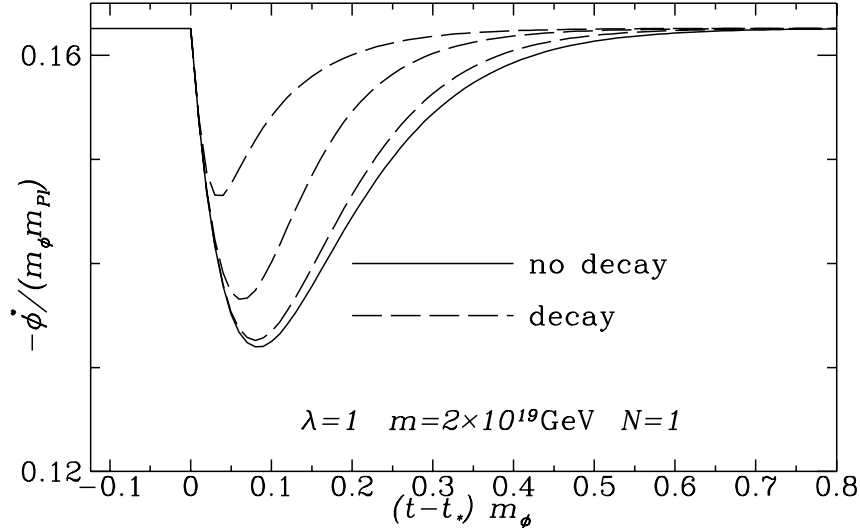
9

FIG. 3. Analytic solutions for $\dot{\phi}$ assuming no decay of the fermion (the solid curve) and with decay parameters $\sqrt{\alpha\lambda\dot{\phi}_*}/m_\phi = 10^3$, 10^2, and 10^1. The feature disappears as $\sqrt{\alpha\lambda\dot{\phi}_*}/m_\phi \to \infty$, and as the quantity approaches zero, we recover the result of no decay.

C. Effect on the Perturbation Spectrum

The simple expression for the perturbation amplitude in terms of H and $\dot{\phi}$ given in the introduction, Eq. (1), must be modified for several reasons. First of all, a correct treatment of the perturbations produced during inflation would involve a variational calculation [32]. The results of this formalism will be reported in another paper. The other reasons the simple expression must be modified can be seen by recalling the derivation of Eq. (1). Ignoring normalization for a moment, the correct starting point is [33]

$$\delta_H \propto \frac{\delta\rho}{\rho + p} \ . \tag{41}$$

First consider the denominator of Eq. (41). If only the inflaton contributes to ρ and p, then $\rho + p = \dot{\phi}^2$, but around the resonance the fermions contribute to ρ and p. An expression for $\rho + p$ that includes this effect is $\rho + p = -\dot{H}m_{Pl}^2/4\pi$.

In the absence of fermion production, the numerator of Eq. (41) is just $\delta\rho = \delta\phi(dV/d\phi)$, with $\delta\phi$ given by quantum fluctuations of the nonzero mode of the inflaton field, $\delta\phi = H/2\pi$. However, fermions produced by the resonance contribute to the fluctuations for two reasons: fluctuations in the fermion field lead to fluctuations in the energy density, and coupling of the produced fermions to the nonzero modes of the inflaton field affect the perturbations. Since the zero mode of the inflaton field still dominates the energy density, these effects are not expected to be large. If they are included, they will increase $\delta\rho$, hence increase the size of the feature in the primordial power spectrum. We will ignore the extra contributions to $\delta\rho$ here, and simply assume that $\delta\rho = \delta\phi(dV/d\phi) = (H/2\pi)(dV/d\phi)$. Finally, one should not use the slow-roll equation ($dV/d\phi = -3H\dot{\phi}$), because $\ddot{\phi}$ may be large when fermions are produced.

In spite of the above considerations, we find that use of the simple expression of Eq. (1) allows reasonably accurate description of the feature in the primordial power spectrum. In the discussion below we describe both analytic and numerical calculations using the following expressions for δ_H:

$$\delta_H = \begin{cases} \dfrac{H^2}{5\pi\dot{\phi}} & \text{analytic} \\[2ex] \dfrac{4H(dV/d\phi)}{15\dot{H}m_{Pl}^2} & \text{numerical} \ . \end{cases} \tag{42}$$

For the analytic approximations we use $H^2 = (8\pi/3)V/m_{Pl}^2$ and $\dot{\phi}$ determined by Eq. (38).

10

With the approximation that the change in $\dot{\phi}$ directly translates into a change in the perturbation spectrum, the character of the features produced in the spectrum can be understood from Eq. (38). Since $\Delta\dot{\phi}$ decays with a characteristic width of $3H_*$, the width of the feature will correspond to less than one e-fold of expansion. For a given change in $\dot{\phi}$ we can estimate the effect on the density perturbation. For the moment, assume the simple result for the density perturbations of Eq. (1). For reasons discussed above, we expect the width of the feature to be less than one e-fold of expansion. Defining a_* to be the value of the scale factor at resonance, a numerical calculation of the spectrum of density perturbations is shown in Fig. 4 as a function of a/a_*. As expected, the width of the feature is less than a single e-fold, and the peak amplitude of the feature corresponds to a peak change in $\dot{\phi}$ estimated from Eq. (39).
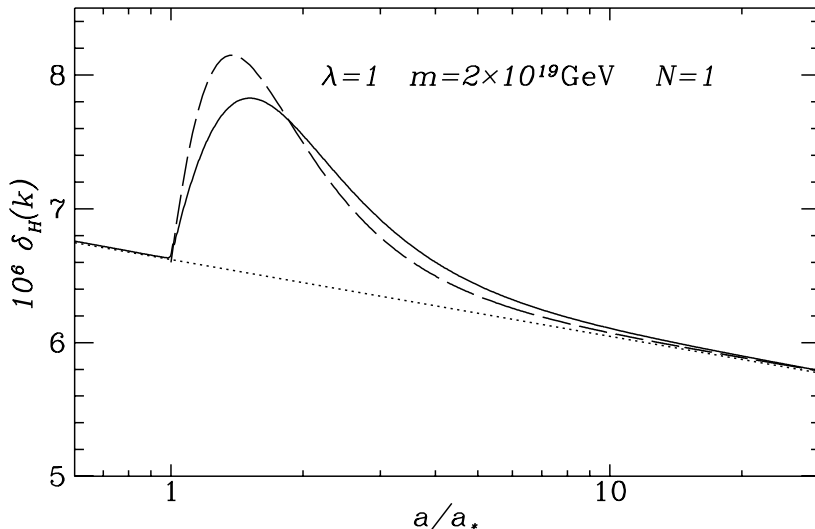
FIG. 4. Resonant particle production produces a peak in the perturbation spectrum as shown in the figure. The solid curve is the numerical result. the dashed curve is the analytic form of Eq. (43). Finally, the dotted curve indicates the power spectrum in the absence of resonant particle creation.

An analytic expression for $\delta_H(k)$ can be obtained using the analytic expression for $\dot{\phi}$. The feature can be approximated by a function of the form

$$\delta_H(k) = \frac{[\delta_H(k)]_{\lambda=0}}{1 - \theta(a - a_*)|\dot{\phi}_*|^{-1}N\lambda n_* H_*^{-1}(a_*/a)^3 \ln(a/a_*)} \ . \tag{43}$$

This expression is also shown in Fig. 4. Clearly it is a very reasonable approximation.

In the comparison between analytic and numerical results presented in this section we have assumed a single fermion species coupled to the inflaton. One might imaging a large number of fermion species coupled to the inflaton. In grand unified theories (GUTs) based upon gauge groups such as $SO(10)$, E_6, and so on, representations of large dimension are easily obtained.

If back reactions are ignored, then the effect of fermion production on the perturbation spectrum is linear in N. However, for large values of $N\lambda^{5/2}$ the back reactions are important. We turn to such a case in the next section.

Before concluding this section we restate the important results: The feature in the spectrum should be about one e-fold in width, and the amplitude of the feature should scale as $N\lambda^{5/2}$ until back reactions become important.

Finally, we note that we can estimate how the change in the perturbation spectrum scales with the inflaton potential. Recalling that $\delta_H = H_*^2/5\pi\dot{\phi}_*$, then

$$\frac{\Delta\delta_H(k)}{\delta_H(k)} = -\frac{\Delta\dot{\phi}_*}{\dot{\phi}_*} = \frac{N\lambda^{5/2}}{6e\pi^3}\frac{3^{1/4}}{8^{3/4}}\frac{1}{\pi^{3/4}}\left(\frac{m_{Pl}^3(dV/d\phi)_*}{V_*^{3/2}}\right)^{1/2} \ , \tag{44}$$

where here we have used the slow-roll equation of motion, $3H_*\dot{\phi}_* = -(dV/d\phi)_*$ and used $H_*^2 = 8\pi V_*/3m_{Pl}^2$. If we recall the approximation

$$\delta_H \simeq \frac{8}{5} \left(\frac{8\pi}{2} \right)^{1/2} \left| \frac{V^{3/2}}{m_{Pl}^3 dV/d\phi} \right| , \tag{45}$$

we see that the term in parenthesis in Eq. (44) is simply proportional to $\delta_H^{-1/2}$. Therefore, if $dV/d\phi$ and V are adjusted for a given δ_H, then the relative amplitude of the feature will be independent of V and $dV/d\phi$. This implies that the results of the paper can be applied to all single-field inflation models, not just the large-field chaotic inflation model we used.

IV. NUMERICAL RESULTS WHEN BACK REACTIONS ARE IMPORTANT

We do not expect a qualitative difference in choosing $\phi_* \simeq 3m_{Pl}$, which corresponds to scales relevant for the CBR, and a lower value of ϕ_*. Numerically it is convenient to work with smaller ϕ_*; in our runs we choose $\phi_* \sim 2m_{Pl}$.

Since we already presented results for the case $\lambda = 1$, $m = 2 \times 10^{19}$ GeV, and $N = 1$, for completeness we also present in Fig. 5 the results for $\phi(t)$ and $H(t)$ in that model.

Note that resonant fermion production has only a marginal effect on the evolution of ϕ and H, but of course it has a large effect on $\dot{\phi}$. Near resonance, $\phi_* \simeq 2m_{Pl}$ and $H_* \simeq 4m_\phi$. The resulting feature in the perturbation spectrum was shown in the previous section.
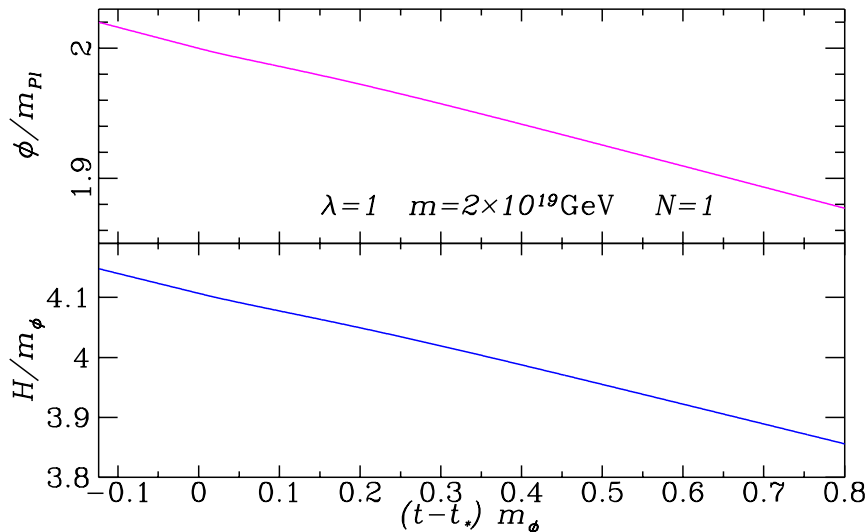

FIG. 5. The evolution of H and ϕ in this model is not noticeably altered by resonant fermion production. Only small inflections in $\phi(t)$ and $H(t)$ are noticeable around the time of resonance, $t \simeq t_*$ where t_* is the time when $\phi = \phi_*$.

Now let's study a model with an even larger amount of fermion creation, where back reactions are quite important. Let's consider the case of $\lambda = 0.316$, $N = 100$, and $m = 6.3 \times 10^{18}$ GeV. As in the previous example, the resonance occurs for $\phi_* \simeq 2m_{Pl}$. The evolution of ϕ and H in this model is shown in Fig. 6. Clearly the evolution of both ϕ and H are modified by resonant particle production. The change in $\dot{\phi}$ is even more dramatic than in the previous example.
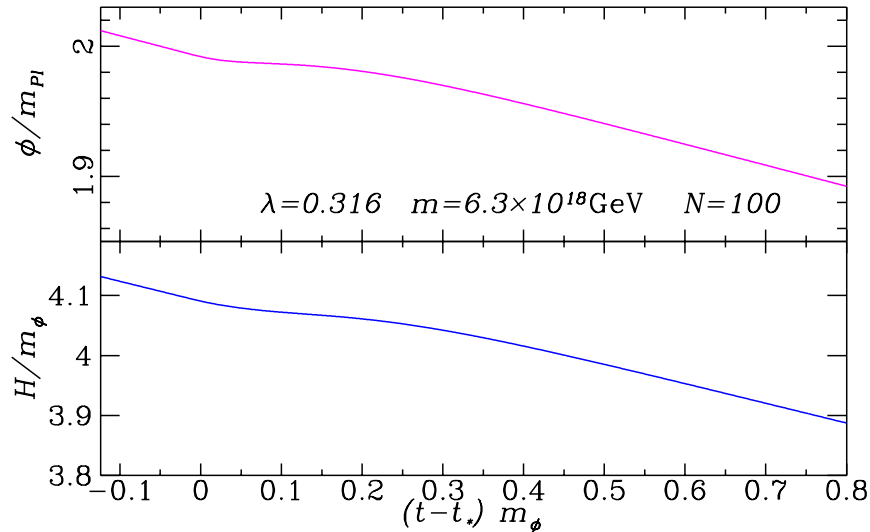
FIG. 6. The evolution of H and ϕ in this model is noticeably altered by resonant fermion production. The flattening in the evolution of ϕ and H begins at $t = t_*$ and continues for a time of about $0.2m_\phi^{-1}$, after which ϕ and H resume decreasing at the rate they would if resonant particle creation had not occurred.

The estimate of the change in $\dot\phi$ in the previous section overestimates the true change. The scaling of Eq. (39) predicts $\max[\Delta\dot\phi]/m_{Pl}m_\phi$ of $100(0.316)^{5/2}$ times the previous estimate of 0.03. This would predict a change in $\dot\phi$ of 0.17, which in fact is larger than $\dot\phi_*$. The back reaction of the created fermions limits the value of $\max[\Delta\dot\phi]$. A numerical calculation of $\dot\phi$ in this model is presented in Fig. 7. While the change in $\dot\phi$ is limited by the back reaction, nevertheless it is quite large.
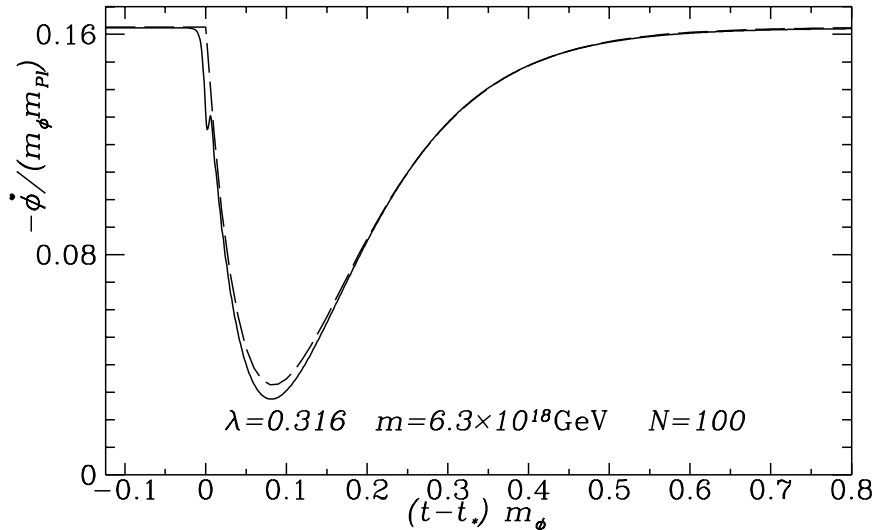

FIG. 7. The change in $\dot\phi$ in this model is modified by the back reaction limiting the energy extracted from the inflaton field. Also shown by the dashed line is the analytic expression of Eq. (46), with A fit to agree with $\max[\Delta\dot\phi]$.

Even though the value of $\max[\Delta\dot\phi]$ is modified by the back reactions, the feature still has the form

$$\Delta\dot\phi(t > t_*) = B(t - t_*)\exp[-3H_*(t - t_*)] , \tag{46}$$

where B is a constant, $B < N\lambda n_*$. The inequality is saturated in the absence of back reactions.

13

A numerical calculation of the primordial perturbation spectrum is shown in Fig. 8 as a function of k/k_*. A physical wavenumber k is related to a by

$$\ln \frac{k}{a_0 H_0} = 62 + \ln \frac{a}{a_*} + \ln \frac{a_*}{a_{\text{end}}} - \ln \frac{10^{16}\,\text{GeV}}{V_k^{1/4}} + \ln \frac{V_k^{1/4}}{V_{\text{end}}^{1/4}} - \frac{1}{3} \ln \frac{V_{\text{end}}^{1/4}}{\rho_{\text{reh}}^{1/4}} \,, \tag{47}$$

where the subscript '0' indicates present values; the subscript 'k' specifies the value when the wave number k crosses the Hubble radius during inflation ($k = aH$); the subscript 'end' specifies the value at the end of inflation; and ρ_{reh} is the energy density of the universe after reheating to the standard hot big bang evolution. The various values of V denote the potential energy density at the indicated epoch. This calculation assumes that instantaneous transitions occur between regimes, and that during reheating the universe behaves as if matter-dominated.

Clearly the exact relationship between a/a_* and a presently observed value of wavenumber is model-dependent. Although the location of the peak in wavenumber (denoted by k_*), cannot be unambiguously stated, the width of the feature in wavenumber is proportional to the width of the feature in the ratio a/a_*, i.e., $k/k_* \propto a/a_*$.

Also shown in Fig. 8 for comparison is a Harrison–Zel'dovich (H–Z) spectrum (spectral index for the primordial spectrum of $n = 0$), and a numerical calculation of the spectrum [assuming the spectrum is given by Eq. (1)] in the model without resonant fermion production. The effective spectral index in the nonresonant inflation model is $n_S = 1 + d \ln \delta_H^2 / d \ln k = 0.96$.

This model produces a huge spike in the primordial power spectrum, more than a factor of three times the underlying spectrum. The feature is fit by a function of the form of Eq. (43):

$$\delta_H(k) = \frac{[\delta_H(k)]_{\lambda=0}}{1 - \theta(k - k_*)8.15A(k_*/k)^3 \ln(k/k_*)} \,. \tag{48}$$

If back reactions are ignored, then $A = |\dot{\phi}_*|^{-1} N \lambda n_* H_*^{-1} / 8.15 \simeq 0.23 N \lambda^{5/2}$. The coefficient A is limited by back reactions to be such that the denominator is positive for $k > k_*$; this implies $A \lesssim 1$. The first model ($N = 1$, $\lambda = 1$) is unaffected by back reactions, and $A = 0.23$. Since back reactions are important in the second model ($N = 100$, $\lambda = 0.316$), the numerical fit ($A = 0.7$) is smaller than expected from the analytic expression $A = 0.23 N \lambda^{5/2} = 1.3$.
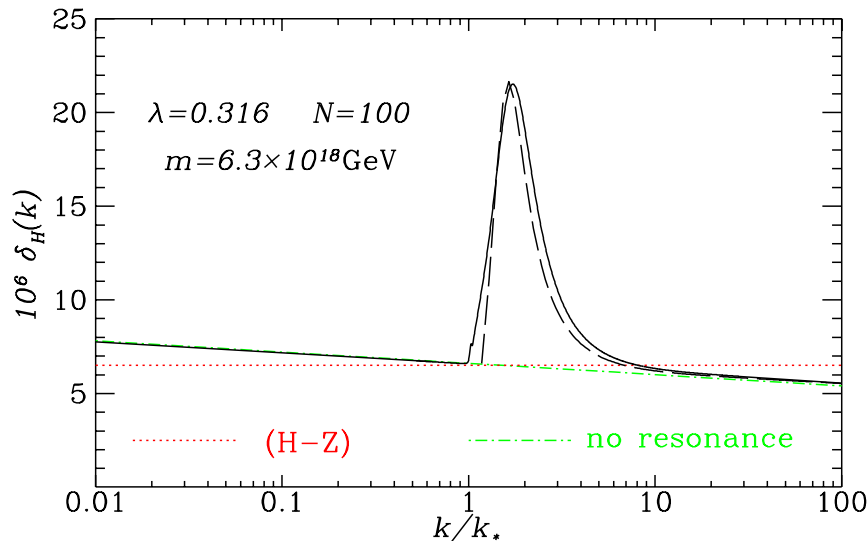

FIG. 8. Resonant particle production produces a peak in the perturbation spectrum as shown by the solid curve in the figure. Shown by a dashed curve is the analytic form of $\delta_H(k)$ in Eq. (48) with the coefficient A chosen to give the best fit. Finally, also shown is a Harrison–Zel'dovich spectrum and the spectrum in the inflation model without resonant particle creation.

V. DISCUSSION AND PROSPECTS FOR DETECTION OF FEATURES

In this paper we have described a reasonably straightforward and simple mechanism to produce features in the spectrum. The features can be characterized by a central location in wavenumber, a width, and an amplitude.

The location of the peak in wavenumber depends on the value of $\phi_* = m/\lambda$. In the large-field inflation model we study, ϕ_* has to be of order two to four times the Planck mass to have any hope of being in the observationally accessible range. Since to produce a noticeable peak λ cannot be too small, m must be of order m_{Pl}.

The narrow width of the feature, less than about a decade in wavenumber (corresponding to about a single e-fold of inflation), is reasonably independent of the model parameters.

The amplitude of the feature does depend on the model parameters, in particular on the combination $N\lambda^{5/2}$. In the first model we presented ($\lambda = 1$, $N = 1$, $m = 2 \times 10^{19}$ GeV), the amplitude of the feature was a factor of 1.3 larger than the underlying spectrum. The second model ($\lambda = 0.316$, $N = 100$, $m = 6.3 \times 10^{18}$ GeV) had a peak increase in the power spectrum of about 3.4 times the non-resonant result, or about 2.6 times the first model. Scaling with $N\lambda^{5/2}$ would predict a peak increase of the second model of 5.6 (rather than 2.6) times that of the first model. The failure of the peak amplitude to scale as predicted is because of the back reaction limiting fermion creation.

Our conclusion is that the characteristic signature of our mechanism is a narrow spike in the power spectrum of width less than a decade in wavenumber and amplitude anywhere from near zero to factors larger than three. An exceedingly good analytic form for the shape of the feature is given in Eq. (48). The peak amplification is $(1 - A)^{-1}$ (recall that $A < 1$). The first model had $A = 0.23$, while the second model had $A = 0.7$.

We now turn to a discussion of how such a feature might be detected in near-future experiments that will measure the present power spectrum. Since the feature produced by resonant particle production is approximately described by a single parameter ($0 < A < 1$), we can estimate the sensitivity of large-scale structure surveys and CBR experiments to a resonant particle production feature. The limit on A of course will depend on the value of k_*.

It is a relatively straightforward exercise to see how a feature in the spectrum would appear in determination of the power spectrum from large-scale structure surveys. The first step is to convert the primordial spectrum, $\delta_H(k)$, which is the amplitude of the perturbation as wavenumber k enters the horizon, to the present-day power spectrum, $P(k)$, which describes the amplitude of the perturbation at a fixed time. This is done by means of the transfer function, $T(k)$ [34]:

$$\frac{k^3}{2\pi^2} P(k) = \left(\frac{k}{aH_0}\right)^4 T^2(k)\delta_H^2(k) \ . \tag{49}$$

The transfer function depends upon a whole range of cosmological parameters (Ω, H_0, Λ, Ω_B, and so on). This expression should be valid in the linear regime of the perturbations, which in comoving wavenumber is approximately $k \lesssim 0.2h\,\mathrm{Mpc}^{-1}$. Features in $\delta_H(k)$ are directly passed through to $P(k)$, and in the linear regime should be straightforward to identify.

For a volume-limited survey, the uncertainty due to cosmic variance and shot noise in the estimated power per mode is [35,36]

$$\frac{\Delta P(k)}{P(k)} = \sqrt{2\frac{(2\pi)^3}{V_S V_k}\left[1 + \frac{1}{\bar{n}P(k)}\right]} \ , \tag{50}$$

where $\bar{n}$ is the mean density of the sample of survey volume V_S and the estimates average over a shell in Fourier space of volume $V_k = 4\pi k^2 \Delta k$. The width of the bins is $\Delta k = 2\pi R^{-1}$, where R is the depth of the survey.

Consider the sensitivity of determinations of the power spectrum expected from the bright red galaxy (BRG) subsample of the SDSS. The volume-limited BRG subsample will include approximately 10^5 galaxies in volume of effective depth $1h^{-1}\,\mathrm{Gpc}$ covering π steradians. It is expected that BRGs are biased by a factor of four in the power spectrum.
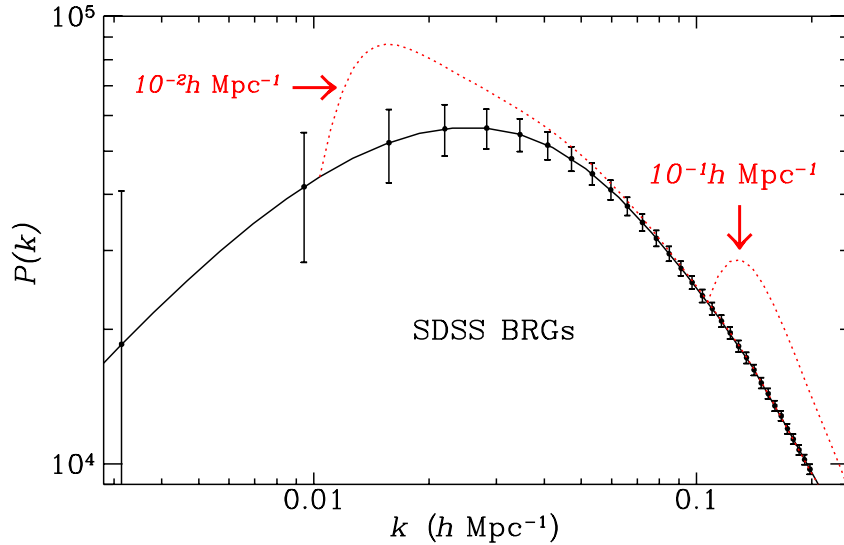
FIG. 9. This figure illustrates the predicted uncertainties [see Eq. (50)] in the power spectrum from the Bright Red Galaxy (BRG) subsample of the Sloan Digital Sky Survey (SDSS). The solid curve is a CDM power spectrum with $\Omega h = 0.25$. The bins in k and the errors are determined by Eq. (50). Also shown by the dotted curves are two features in the power spectrum at the indicated values of k_* and for the same value of $A = 0.23$ [see Eq. (48)].

The sold curve in Fig. 9 is generated assuming a Harrison–Zel'dovich primordial spectrum and a CDM transfer function. The points are in wavenumber bins with errors taken from Eq. (50). The two dotted curves are power spectra with features of the form that would be generated by resonant particle production. In the form of Eq. (48), the two examples have $k_* = 10^{-2}h\,\mathrm{Mpc}^{-1}$ and $k_* = 10^{-1}h\,\mathrm{Mpc}^{-1}$ and both have $A = 0.23$ (the result of the model with $\lambda = 1$, $N = 1$, and $m = 2 \times 10^{19}\,\mathrm{GeV}$). Clearly either feature would be detected.
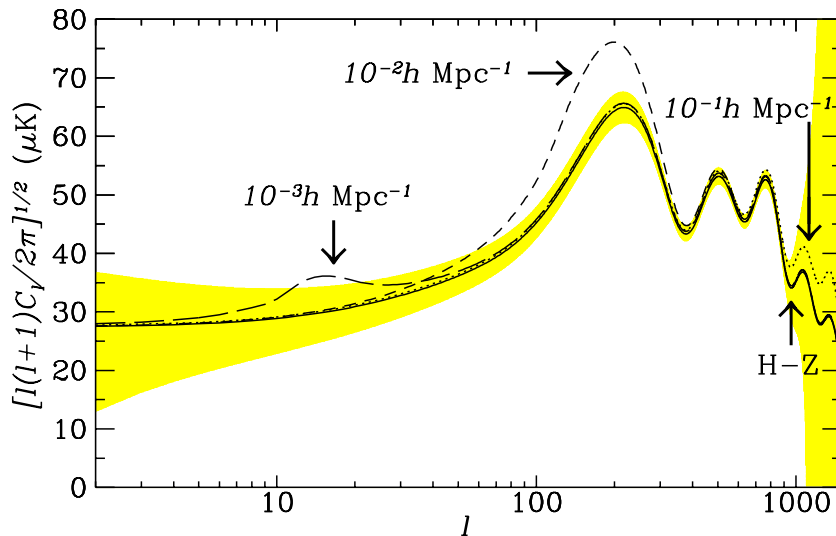

FIG. 10. The angular power spectrum calculated for a featureless Harrison–Zel'dovich CDM model (solid curve marked H–Z) and models with features produced by resonant particle production with $A = 0.23$ and the indicated values of k_* [see Eq. (48)]. The cosmological parameters are identical for all models. The shaded area indicates the expected uncertainty in the C_l's from the MAP satellite. The models have all been normalized to the same value of C_2.

Features in the primordial power spectrum will also affect the CBR temperature fluctuations. The CBR temperature

16

fluctuations can be expanded in spherical harmonics, $\delta T/T = \sum_l \sum_m a_{lm} Y_{lm}(\theta, \phi)$ ($2 < l < \infty$ and $-l < m < l$). The anisotropies are described by the angular power spectrum, $C_l = \langle |a_{lm}|^2 \rangle$, as a function of multipole number l.

The amplitude of the perturbation spectrum at a given wavenumber k contributes to the angular power spectrum in a range of l, so the effect of a narrow feature is spread over several values of l. The angular power spectrum is easily calculated using CMBFAST [37]. The result of a sample model calculations is shown in Fig. 10. The angular power spectrum resulting from a featureless power-law spectrum (Harrison–Zel'dovich) is shown by the solid curve. Also shown for comparison are three other models with features in the primordial power spectrum of the form in Eq. (48), with $A = 0.23$ and $k_* = 10^{-3} h\,\mathrm{Mpc}^{-1}$, $10^{-2} h\,\mathrm{Mpc}^{-1}$, and $10^{-1} h\,\mathrm{Mpc}^{-1}$.

The CBR is sensitive to the power spectrum in the interval from about $10^{-4} h\,\mathrm{Mpc}^{-1}$ to $10^{-1} h\,\mathrm{Mpc}^{-1}$. For $k_* < 10^{-3} h\,\mathrm{Mpc}^{-1}$, a feature with $A < 0.23$ will be too small to be detected because cosmic variance will be large at small l. For $k_* \sim 10^{-2} h\,\mathrm{Mpc}^{-1}$, the largest effect will be near the first Zel'dovich peak and could have an effect on determination of the geometry of the universe from the location of the peak. If $k_* \sim 10^{-1} h\,\mathrm{Mpc}^{-1}$, the largest effect will be in the region of the secondary peaks. If k_* is much larger than $10^{-1} h\,\mathrm{Mpc}^{-1}$, the effect will be out of the range of CBR sensitivity.

A meaningful detection limit is hard to quote; the limiting value of A depends on k_* (among other things). In Fig. 11 we indicate by the shaded regions the values of A that will differ more than a 2σ from the best-fit featureless power-law spectrum expected to be determined by SDSS and MAP.

The feature around $k_* = 3 \times 10^{-3} h\,\mathrm{Mpc}^{-1}$ in the SDSS limit is due to the feature falling between the widely spaced bins in that region. In the figure we have assumed the normalization will be set by CBR determinations, i.e., the normalization is a free parameter for the MAP limits, but not for the SDSS limits. In principle, the region of sensitivity could extend to k_* greater than $0.1 h\,\mathrm{Mpc}^{-1}$ if the evolution of the power spectrum in the mildly nonlinear regime was completly understood.

The form of the limit from MAP around $k_* \sim 3 \times 10^{-2} h\,\mathrm{Mpc}^{-1}$ is due to the fact that the spectral feature in that region falls in the region of the Zel'dovich peaks.

For $10^{-2} \lesssim k_* \lesssim 10^{-1} h\,\mathrm{Mpc}^{-1}$, the smallest A that has a 2σ effect is about 6×10^{-3}.[6] This would correspond to the limit

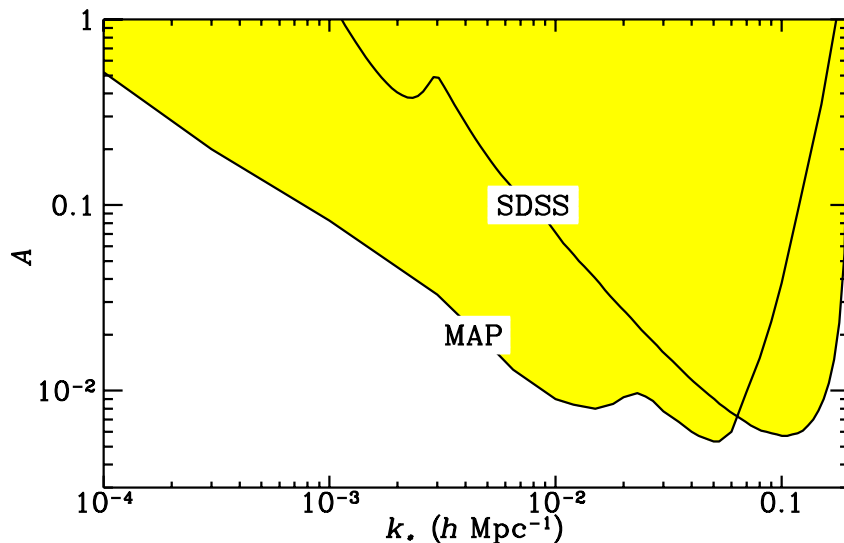$$\lambda < 0.2/N^{2/5} \ . \tag{51}$$

FIG. 11. The shaded region will produce a 2σ change in the matter power spectrum with the expected sensitivity expected for the SDSS–BRG subsample and the MAP CBR satellite mission.

---

[6]Here we are not saying that $A = 6 \times 10^{-3}$ would be cleanly detectable, only that a featureless power-law spectrum would not be a good fit.

The correct way to interpret this limit is that if it is violated, the feature in the spectrum produced by resonant particle production has the potential of being detected in large-scale structure surveys.

Again, any limit on A will depend on k_*. For k_* near $10^{-2}h\,\mathrm{Mpc}^{-1}$ and A as small as 0.01, the effect of resonant particle production will be noticeable. For larger A it is possible that the feature could be noticeable in both CBR and large-scale structure surveys.

VI. CONCLUSIONS

For the most part, analysis involving the power spectrum assumes that it is a featureless power law. Occasionally one includes smooth variation in the spectral index, but usually retaining the assumption that the power spectrum is featureless.

In this paper we presented a reasonably straightforward scenario for producing a spike (or several spikes) in the power spectrum. While analysis assuming a featureless power spectrum is certainly a reasonable first step, it would be wise to keep in mind that when doing so one is making an approximation about the dynamics during inflation that may not be true.

Let us now elaborate about the particle physics motivations of our work. When speaking about a 'model of inflation', the phrase is actually used by the community in two rather different ways. At the simplest level a 'model of inflation' is taken to mean a form for the potential, as a function of the fields giving a significant contribution to it. In single-field models this is just the inflaton field ϕ. If one knows $V(\phi)$ and the field value at the end of inflation, this allows one to calculate the spectrum of density perturbations.

At a deeper level, one thinks of a 'model of inflation' as something analogous to the Standard Model of particle interactions [38]. One imagines that nature has chosen some extension of the Standard Model, and that the scalar fields relevant for inflation are part of that model. In this sense a 'model of inflation' is more than merely a specification of the the potential of the relevant fields. It will provide answers to some fundamental questions such as whether the relevant fields and interactions have already been invoked in some other context and, if so, what are the mass parameters and the coupling constants in the sectors coupled to the inflaton field(s).

Of course, it would have been wonderful if inflation already dropped out of the Standard Model of particle physics, but sadly that is not the case. On the contrary, it seems very likely that the physics responsible for an inflationary stage during the early evolution of the universe is due to some particle physics model whose typical energy is much larger than the weak scale and whose field values during inflation may be larger than the Planck mass.

Well studied extensions of the Standard Model, such as supergravity and superstring theories, have the Planck mass as a fundamental scale. The exact motivations and goals of these theories beyond the Standard Model might be different, but for many applications to cosmology they have several common features. For instance, they contain in the spectrum particles with Planckian masses and are formulated in extra-dimensions. These extra-dimensions are compact and smaller than the three large spatial dimensions. It is therefore possible to dimensionally reduce the system and obtain and 'effective' 3+1 dimensional theory leaving behind a tower of Kaluza-Klein (KK) states (pyrgons [39]) whose mass is of the order of the inverse size of the extra dimension. Since the extra dimensions are expected to have a size characteristic of the Planck length, these KK states therefore have Planckian masses. Furthermore, these states are largely degenerate, the level of degeneracy depending upon the geometrical structure of the compact space. It is therefore quite natural to expect that a large number of fermions with the same mass, approximately m_{Pl}, couple to the sector responsible for the inflationary stage. In the simplest approach, this degeneracy factor may be accounted for by the parameter N we have used in the previous sections. Since N may be easily of the order of 100, a detectable signature in the spectrum may be present even in the case of small Yukawa couplings. Thus, the observation of a spike (or several spikes) in the power spectrum of the density perturbation may help us in understanding the features of the inflaton sector and thus testing Planckian physics. In the absence of any other experimental signature, this is certainly very intriguing.

ACKNOWLEDGMENTS

[1] E. Gaztañaga and C. M. Baugh, Mon. Not. Roy. Astron. Soc **294**, 801, 229 (1998).

[2] T. J. Broadhurst, R. S. Ellis, D. C. Koo, and A. S. Szalay, Nature (London), **343**, 726 (1990); T. Broadhurst and A. H. Jaffe, astro-ph/9904348.

[3] J. Einasto *et al.*, Nature (London) **385**, 139 (1997); J. Einasto *et al.*, Mon. Not. Roy. Astron. Soc **289**, 801, 813 (1997); J. Einasto, Gravitation and Cosmol. **4**, Suppl., 110 (1998).

[4] M. Geller, M. J. Kurtz, G. Wegner, Astron,. J. **114**, 2205 (1997).

[5] D. L. Tucker, A. Oemler, Jr., R. P. Kirshner, R. P. Lin, S. A. Shectman, S. D. Landy, P. L. Schechter, V. Müller, V. Gottlöber, and J. Einasto, Mon. Not. R. Astron. Soc. **285**, L5 (1997).

[6] D. J. Eisenstein, W. Hu, J. Silk, and A. S. Szalay, Astrophys. J. **494**, L1 (1998).

[7] D. La and P. J. Steinhardt, Phys. Rev. Lett. **62**, 376 (1989).

[8] F. Occhionero and L. Amendola, Phys. Rev. D **50**, 4846 (1994); L. Amendola, C. Baccigalupi, and F. Occhionero, Astrophys. J. **492**, L8 (1998).

[9] J. A. Adams, G. G. Ross, and S. Sarkar, Nucl. Phys. **B503**, 405 (1997); F. Arrio-Barandels, J. Einasto, J. Gottlöber, S. Müller, and A. A. Starobinsky, J. Exp. Theor. Phys. **66**, 397 (1997).

[10] A. A. Starobinsky, Grav. Cosmol. **4**, 88 (1998).

[11] E. W. Kolb and M. S. Turner, *The Early Universe*, (Addison-Wesley, Menlo Park, Ca., 1990).

[12] G. Jungman, M. Kamionkowski, A. Kosowsky, and D. N. Spergel, Phys. Rev. D **54**, 1332 (1996); M. Zaldarriaga, D. N. Spergel, and U. Seljak, Astrophys. J. **488**, 1 (1997); J. R. Bond, G. Efstathiou, and M. Tegmark, Mon. Not. Roy. Astron. Soc. **291**, L33 (1997).

[13] D. J. Eisenstein, W. Hu and M. Tegmark, Astrophys. J. **518**, 2 (1999)

[14] P. J. E. Peebles and J. T. Yu, Astrophys. J. **162**, 815 (1970); R. Sunyaev and Ya. B. Zel'dovich, Astro. and Space Sci. **7**, 3 (1970); J. A. Holtzman, Astrophys. J. Suppl. **71**, 1 (1989); W. Hu and N. Sugiyama, Astrophys. J. **471**, 542 (1996); D. J. Eisenstein and W. Hu, Astrophys. J. **496**, 605 (1998).

[15] 2dF: http://www.mso.anu.edu.au/ colless/2dF/.

[16] SDSS: http://www.sdss.org/.

[17] M. Tegmark, Phys. Rev. Lett. **79** 3806 (1997); A. Meiksin, M. White, and J. A. Peacock, Mon. Not. R. Astron. Soc. **304**, 851 (1999).

[18] Y. Wang, D. N. Spergel, and M. Strauss, Astrophys. J. **510**, 20 (1999).

[19] J. E. Lidsey, A. R. Liddle, E. W. Kolb, E. J. Copeland, T. Barreiro, and M. Abney, Rev. Mod. Phys. **69**, 373 (1997).

[20] E. J. Copeland, I. J. Grivell, E. W. Kolb, and A. R. Liddle, Phys. Rev. D **58**, 043002 (1998).

[21] I. J. Grivell and A. R. Liddle, astro-ph/9906327.

[22] G. F. Giudice, M. Peloso, A. Riotto, and I. I. Tkachev, JHEP **9908**, 014 (1999) [hep-ph/9905242].

[23] S. G. Mamaev, V. M. Mostepanenko, and V. M. Frolov, Sov. J. Nucl. Phys. **23**, 592 (1976).

[24] V. A. Kuzmin and I. I. Tkachev, Phys. Rev. **D59**, 123006 (1999).

[25] A. A. Grib, S. G. Mamaev, and V. M. Mostepanenko, *Quantum Effects in Strong External Fields*, Atomic Energy Press, Moscow (1980).

[26] J. Baacke, K. Heitmann, and C. Patzold, Phys. Rev. D **58**, 125013 (1998).

[27] R. Kallosh, L. Kofman, A. Linde, A. Van Proeyen, hep-th/9907124; G.F. Giudice, I. Tkachev, A. Riotto, JHEP 9908:009 (1999) [hep-ph/9907510].

[28] P. B. Greene and L. Kofman, Phys. Lett. **B448**, 6 (1999).

[29] N. D. Birrell and P. C. W. Davies, Quantum Fields in Curved Space, (Cambridge Univ. Press, Cambridge, 1982).

[30] L. Kofman, A. Linde, A. A. Starobinsky, Phys. Rev. **D56**, 3258 (1997).

[31] D. J. H. Chung, hep-ph/9809489.

[32] For a review, see V. F. Mukhanov, H. A. Feldman, and R. H. Brandenberger, Phys. Rep. **215**, 203 (1992).

[33] J. M. Bardeen, P. J. Steinhardt, and M. S. Turner, Phys. Rev. D **28**, 679 (1983).

[34] G. P. Efstathiou, in *Physics of the Early Universe*, (SUSSP Publications, Edinburgh, 1990), eds. A. T. Davies, A. Heavens, and J. Peacock.

[35] H. Feldman, N. Kaiser, and J. Peacock, Astrophys. J. **426**, 23 (1994).

[36] M. S. Vogeley, in *Ringberg Workshop on Large-Scale Structure*, (Kluwer, Amsterdam, 1998), ed. D. Hamilton.

[37] U. Seljak and M. Zaldarriaga, Astrophys. J. **469**, 437 (1996).

[38] D.H. Lyth and A. Riotto, Phys. Rep. **314**, 1 (1999).

[39] E. W. Kolb and R. Slansky, Phys. Lett **135B**, 378 (1984).